Circuit Models to Study the Radiated and Conducted Susceptibilities of Multiconductor Shielded Cables Connected to Nonlinear Loads

Mohamed Saih[1*], Zahra Bouzidi[2] ,Youssef Rhazi[3]
Laboratory of Automatic, Energy Conversion and Microelectronics, Faculty of Sciences and Technology, University of Sultan -1
. Moulay Slimane, Beni-Mellal, Morocco
(Email: saih.mohamed2@gmail.com (Corresponding author
, Laboratory of Electrical Systems and Telecommunications, Faculty of Sciences and Technology, CadiAyyad University -2
. Marrakech, Morocco
Email: zahra.bouzidi@edu.uca.ma
Laboratory of Automatic, Energy Conversion and Microelectronics, Faculty of Sciences and Technology, University of Sultan -3
. Moulay Slimane, Beni-Mellal, Morocco
Email: rhazi.lastid@gmail.com

Received: February 2021 Revised: May 2021 Accepted: July 2021

ABSTRACT:
This paper presents Circuit Models which are developed for the analysis of the radiated and conducted susceptibilities of nonuniform shielded coaxial cables. In order to obtain the voltage and current distributions, a two-step procedure is performed. First, the cables are subdivided into several uniform sections. Second, the Branin's mode is used to obtain the voltage and current distributions. This model can be used directly in the analysis of both time-domain and frequency-domain, and it has the ability to be used without the need of setting the preconditions for charges which are applied to its ends. In this paper, three examples of applications in the time and frequency domains are presented in order to validate our model. The first example focuses on a coaxial shielded cable to analyze both the conducted and radiated immunity, while the second example focuses on a nonuniform coaxial shielded cable. The third example presents a complex configuration of a coaxial cable which has been exposed to an electromagnetic field incident. Finally, the performed simulations and obtained results will be thoroughly described and analyzed.

KEYWORDS: Shielded Coaxial Cables, Branin's Model, Radiated Susceptibility, Conducted Susceptibility, Incident Electromagnetic Field.

1. INTRODUCTION

Coaxial shielded cables are often inserted in wired communication systems to protect the data being transferred through the cable from degradation by electromagnetic interference (EMI) exposure. Electromagnetic field coupling from ambient radiation onto coaxial shielded cables can reduce the performance of a circuit or even cease its functioning altogether. Therefore, the prediction of the susceptibility of coaxial shielded cables will be advantageous for a good optimization of system design.

Many techniques are established to determine the equations of the lines, in both the frequency and time domains. One of these techniques consists of the traditional cascading technique which enables line demonstrating in the form of RLCG (Resistance, Inductance, Capacitance and Conductance) equivalent circuit model. This technique can also be used in the case of Multiconductor Transmission Lines (MTLs) [1], however this would make the equivalent scheme more complicated. In addition, it ends up in oscillations to temporal responses and also requires a considerable time for calculation, rendering it pointless.

Recently, Circuit models for MTLs with or without shields have been an essential subject among research. One of the examples is the method that Caniggia and Maradei [2] presented in their latest research and which has enabled them to analyze the conducted immunity of coaxial cables. In addition, they have also introduced spice models in order to study both the radiated and the conducted immunity of lossless shielded cables [3]. The disadvantage of this method is that it requires the use of the inverse Fourier transform to execute the time-domain results. In the last few years, using Spice models, a fastidious focused on examination has been performed to analyze the conducted and the radiated susceptibilities of lossless [4], [5] and lossy [6], [7] shielded coaxial cables. The main reasons for using these models is the probability of using them as a part of the time and frequency domains, either with linear or nonlinear loads.

Paper type: Research paper
DOI: https://doi.org/10.52547/mjee.16.1.9
How to cite this paper: M. Saih, Z. Bouzidi and Y. Rhazi,"**Circuit Models to Study the Radiated and Conducted Susceptibilities of Multiconductor Shielded Cables Connected to Nonlinear Loads**", Majlesi Journal of Electrical .Engineering, Vol. 16, No. 1, pp. 9-17, 2022

In all of the above analyses, it can be observed that all the models that are used have only studying uniform shielded cables. However, in practice there might be also many cases where the cables are nonuniform.

In this study, an equivalent circuit model is presented for the analysis of both the conducted and the radiated susceptibilities of nonuniform shielded coaxial cables. Regardless of the types of loads, these models can be applied to study both the time and frequency domains. The results and interpretation of this simulation will be presented and compared with those from other methods.

2. DESCRIPTION OF SHIELDED COAXIAL CABLE

2.1. Model of Shielded Coaxial Cable

The telegrapher's equations for a coaxial shielded cable in the presence of external electromagnetic radiation, as shown in Fig. 2 can be described by[4], [6]:

Outer system (Shield)

$$\begin{cases} \dfrac{\partial V_{sh}(z,t)}{\partial z} + L_{sh}\dfrac{\partial I_{sh}(z,t)}{\partial t} + R_{sh} I_{sh}(z,t) = V_f(z,t) \\ \dfrac{\partial I_{sh}(z,t)}{\partial z} + C_{sh}\dfrac{\partial V_{sh}(z,t)}{\partial t} + G_{sh} V_{sh}(z,t) = I_f(z,t) \end{cases} \quad (1)$$

Inner system (wire)

$$\begin{cases} \dfrac{\partial V_w(z,t)}{\partial z} + L_w\dfrac{\partial I_w(z,t)}{\partial t} + R_w I_w(z,t) = Z_t I_{sh}(z,t) \\ \dfrac{\partial I_w(z,t)}{\partial z} + C_w\dfrac{\partial V_w(z,t)}{\partial t} + G_w V_w(z,t) = 0 \end{cases} \quad (2)$$

Where, C_{sh}, L_{sh}, G_{sh} and R_{sh} are the per-unit-lenght -pul- capacitance, inductance, conductance and resistance of the outer system (shield), respectively. $V_{sh}(z,t)$ and $I_{sh}(z,t)$ represent the voltage and the current of the outer system, while $V_w(z,t)$ and $I_w(z,t)$ are the voltage and the current of the inner system. C_w, L_w, G_w and R_w are the per-unit-lenght -pul- capacitance , inductance, conductance and resistance of the inner system (wire), respectively. Z_t represents the transfer impedance, and it is given by the following expression [8]

$$Z_t = Z_d + j\omega L_t \quad (3)$$

Z_d and L_t represent the diffusion term and the inductance which aperture-penetration effects in a braided-shield coaxial cable, respectively. The formulation of both Z_d and L_t in terms of the braid weave parameters can refer to the literature [9]. In this work, we applied a simplified formulation [6]

$$Z_t = R_t + j\omega L_t \quad (4)$$

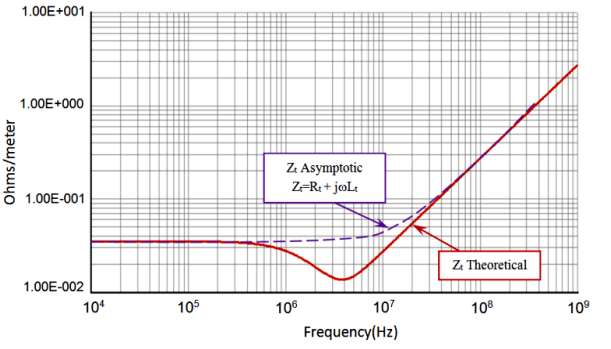

Fig. 1. Transfer impedance of a braided shield.

Where, R_t is the constant per-unit-length transfer resistance of the shield. The impact of external radiation is represented by $V_f(z,t)$ and $I_f(z,t)$, which are distributed sources (forcing functions). The comparison of the transfer impedance magnitude between the asymptotic and theoretical results is shown in Fig.1. Taylor et al. , Agrawal et al., and Rachidi [10], [11] have developed a three different equivalent coupling formulations for the evaluation of the voltages induced by an external electromagnetic field on a transmission line. The formula defined by Taylor is utilized here. In this model, the distributed sources are characterized with regard to the vertical and horizontal components of the incident electric field, that are provided by

$$V_f = \left\lfloor E_z^{inc}(h,z,t) - E_z^{inc}(0,z,t) \right\rfloor - \frac{\partial}{\partial z}\int_0^h E_x^{inc}(x,z,t)dx \quad (5a)$$

$$I_f = -C\frac{\partial}{\partial t}\int_0^h E_x^{inc}(x,z,t)dx \quad (5b)$$

Where, h is the height of the line, and $E_z^{inc}(h,z,t)$ and $E_x^{inc}(x,z,t)$ are the horizontal and vertical components of the incident electric field, respectively. The transmission lines can be treated accurately, eventhough they are nonuniform, using cascaded series of segments of uniform lines, with different characteristic parameters, as shown in Fig. 5. In addition, the circuit model is made for each portion of the uniform line using Branin's model [6]. When the line is above a ground plane, as exhibited in Fig.4, the all-out incident field is the sum total of the original field and the ground-reflected field.

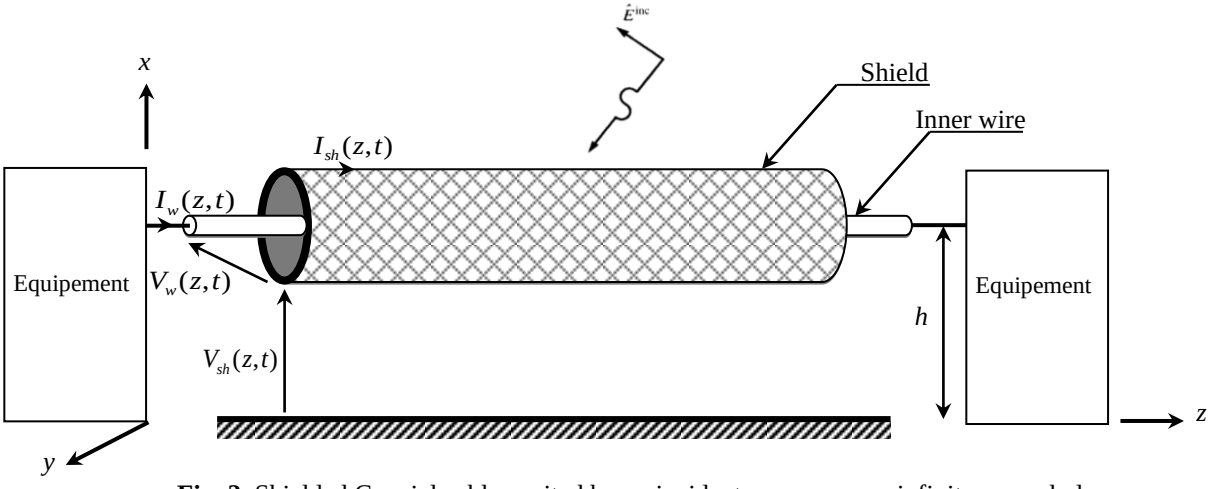

Fig. 2. Shielded Coaxial cable excited by an incident wave over an infinite ground plane.

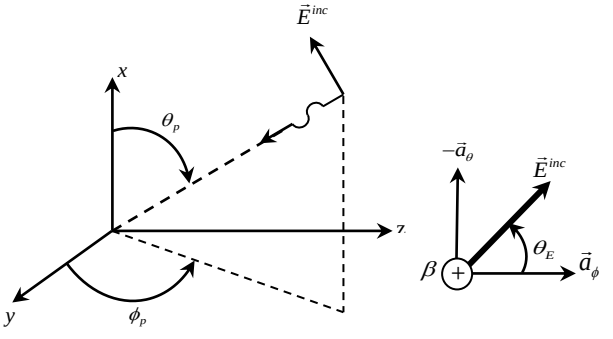

Fig. 3. The parameters describing the incident field in the case of a uniform plane wave.

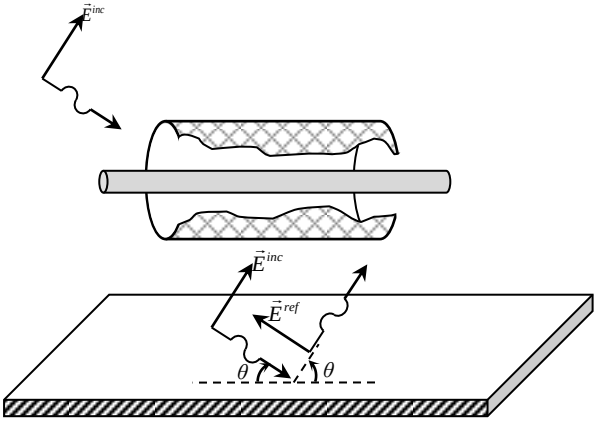

Fig. 4. The representation of total field : the original field (incident) -and the reflected field (image)

$$\vec{E}_{total}^{inc} = \vec{E}^{inc} + \vec{E}^{ref} \tag{6}$$

The field components are as follows

$$\vec{E}^{inc}(x,y,z,\omega) = E_0(e_x\vec{a_x} + e_y\vec{a_y} + e_z\vec{a_z}) \times e^{-j\beta_x x}e^{-j\beta_y y}e^{-j\beta_z z} \tag{7}$$

$$\vec{E}^{ref}(x,y,z,\omega) = E_0(e_x\vec{a_x} - e_y\vec{a_y} - e_z\vec{a_z}) \times e^{j\beta_x x}e^{-j\beta_y y}e^{-j\beta_z z} \tag{8}$$

$$\vec{E}_{total}^{inc} = \vec{E}^{inc} + \vec{E}^{ref} = E_{total_x}^{inc}\vec{a}_x + E_{total_y}^{inc}\vec{a}_y + E_{total_z}^{inc}\vec{a}_z \tag{9}$$

$$E_{total_x}^{inc} = 2E_0e_x\cos(\beta_x x)e^{-j\beta_y y}e^{-j\beta_z z} \tag{10a}$$

$$E_{total_y}^{inc} = -2jE_0e_y\sin(\beta_x x)e^{-j\beta_y y}e^{-j\beta_z z} \tag{10b}$$

$$E_{total_z}^{inc} = -2jE_0e_z\sin(\beta_x x)e^{-j\beta_y y}e^{-j\beta_z z} \tag{10c}$$

Where, e_x, e_y and e_z denote the components of the incident electric field vector according to x, y , and z axes, and are written as:

$$\begin{cases} e_x = \sin\theta_E\sin\theta_P \\ e_y = -\sin\theta_E\cos\theta_P\cos\phi_P - \cos\theta_E\sin\phi_p \\ e_z = -\sin\theta_E\cos\theta_P\sin\phi_P + \cos\theta_E\cos\phi_P \\ e_x^2 + e_y^2 + e_z^2 = 1 \end{cases} \tag{11}$$

We describe the polarization sort by the angle θ_E . If it equals zero, the polarization is horizontal but if it is equal to 90°, the polarization is vertical. In addition, the elevation is decided by the angle θ_p, with respect to the ground, which is referred to as the incident angle. The

angle ϕ_p provides the propagation direction relative to the axis O, as appeared in Fig.3.

β_x , β_y and β_z represent the phase constant, and are given by:

$$\begin{cases} \beta_x = -\beta\cos\theta_P = -\dfrac{\omega}{v_0}\sqrt{\mu_r\varepsilon_r}\cos\theta_P \\ \beta_y = -\beta\sin\theta_P\cos\phi_P = -\dfrac{\omega}{v_0}\sqrt{\mu_r\varepsilon_r}\sin\theta_P\cos\phi_P \\ \beta_z = -\beta\sin\theta_P\sin\phi_P = -\dfrac{\omega}{v_0}\sqrt{\mu_r\varepsilon_r}\sin\theta_P\sin\phi_P \end{cases} \quad (12)$$

Where, v_0 is the phase velocity in the space,

Now let us consider the case where the line is nonuniform. In this case, the cable is subdivided into n fragment of a similar length $\Delta z=\lambda/10$.

The general solution for the line voltages and currents given in (1) and (2), for each section, is as follows

$$\begin{cases} V_{sh}(z_0) = Z_{csh}I_{sh}(z_0) + \underbrace{e^{-\gamma_{sh}\Delta z}[V_{sh}(z_0+\Delta z) - Z_{csh}I_{sh}(z_0+\Delta z)]}_{V_{rsh}} \\ V_{sh}(z_0+\Delta z) = -Z_{csh}I_{sh}(z_0+\Delta z) + \underbrace{e^{-\gamma_{sh}\Delta z}[V_{sh}(z_0) + Z_{csh}I_{sh}(z_0)]}_{V_{ish}} \end{cases} \quad (13)$$

$$\begin{cases} V_w(z_0) = Z_{cw}I_w(z_0) + \left(\underbrace{\begin{array}{l} e^{-\gamma_w\Delta z}[V_w(z_0+\Delta z) \\ -Z_{cw}I_w(z_0+\Delta z) \\ -Z_tI_{sh}(z_0+\Delta z)] \end{array}}_{V_{rw}}\right) \\ V_w(z_0+\Delta z) = -Z_{cw}I_w(z_0+\Delta z) \\ \qquad + \underbrace{e^{-\gamma_w\Delta z}[V_w(z_0) + Z_{cw}I_w(z_0)]}_{V_{iw}} \\ \qquad + Z_tI_{sh}(z_0+\Delta z) \end{cases} \quad (14)$$

In equations (13) and (14), Z_{csh} and Z_{cw} denote the characteristic impedance of the outer and the inner system, respectively.

$$\begin{cases} Z_{csh} = \sqrt{\dfrac{(R_{sh}+j\omega L_{sh})}{j\omega C_{sh}}} \\ Z_{cw} = \sqrt{\dfrac{(R_w+j\omega L_w)}{j\omega C_w}} \end{cases} \quad (15)$$

By using the first term of the Taylor series expansion, Eq. (15) then becomes:

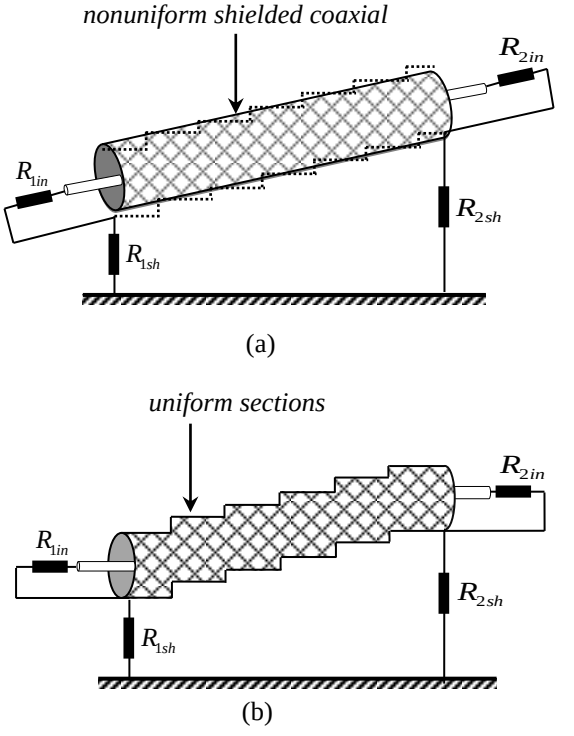

Fig. 5. (a) Coaxial line is approximated by cascaded series of sections of (b) uniform lines.

$$\begin{cases} Z_{csh} = R_p + \dfrac{1}{jC_p\omega} \\ Z_{cw} = R_j + \dfrac{1}{jC_j\omega} \end{cases} \quad (16)$$

Where

$$R_p = \sqrt{\frac{L_{sh}}{C_{sh}}} \quad \text{and} \quad C_p = \frac{2L_{sh}}{R_{sh}R_p} \quad (17)$$

$$R_j = \sqrt{\frac{L_w}{C_w}} \quad \text{and} \quad C_j = \frac{2L_w}{R_wR_j} \quad (18)$$

In this case, the characteristic impedance can be viewed as resistance and capacity connected in series, as shown in Fig. 6. γ_{sh} and γ_w are the propagation constants of the outer and the inner system, respectively, and defined as

$$\gamma_{sh} = \alpha_{sh} + j\beta_{sh} = \sqrt{(R_{sh}+j\omega L_{sh})\,j\omega C_{sh}} \quad (19a)$$

$$\gamma_w = \alpha_w + j\beta_w = \sqrt{(R_w+j\omega L_w)\,j\omega C_w} \quad (19b)$$

The equivalent circuit represented in Fig. 7 can be

obtained from the equations (13), (14) and (16). Additionally, due to the radiated immunity, the generators 'forced' of voltage and current IFT and VFT, which represent the distribution sources, ought to be included at the terminal.

They are also specified by the accompanying equations [12]

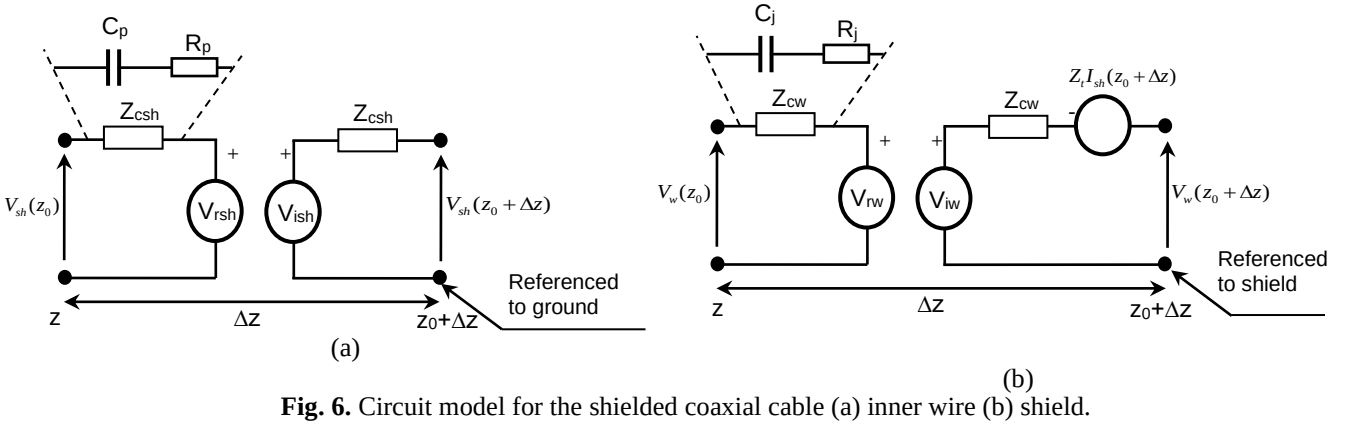

Fig. 6. Circuit model for the shielded coaxial cable (a) inner wire (b) shield.

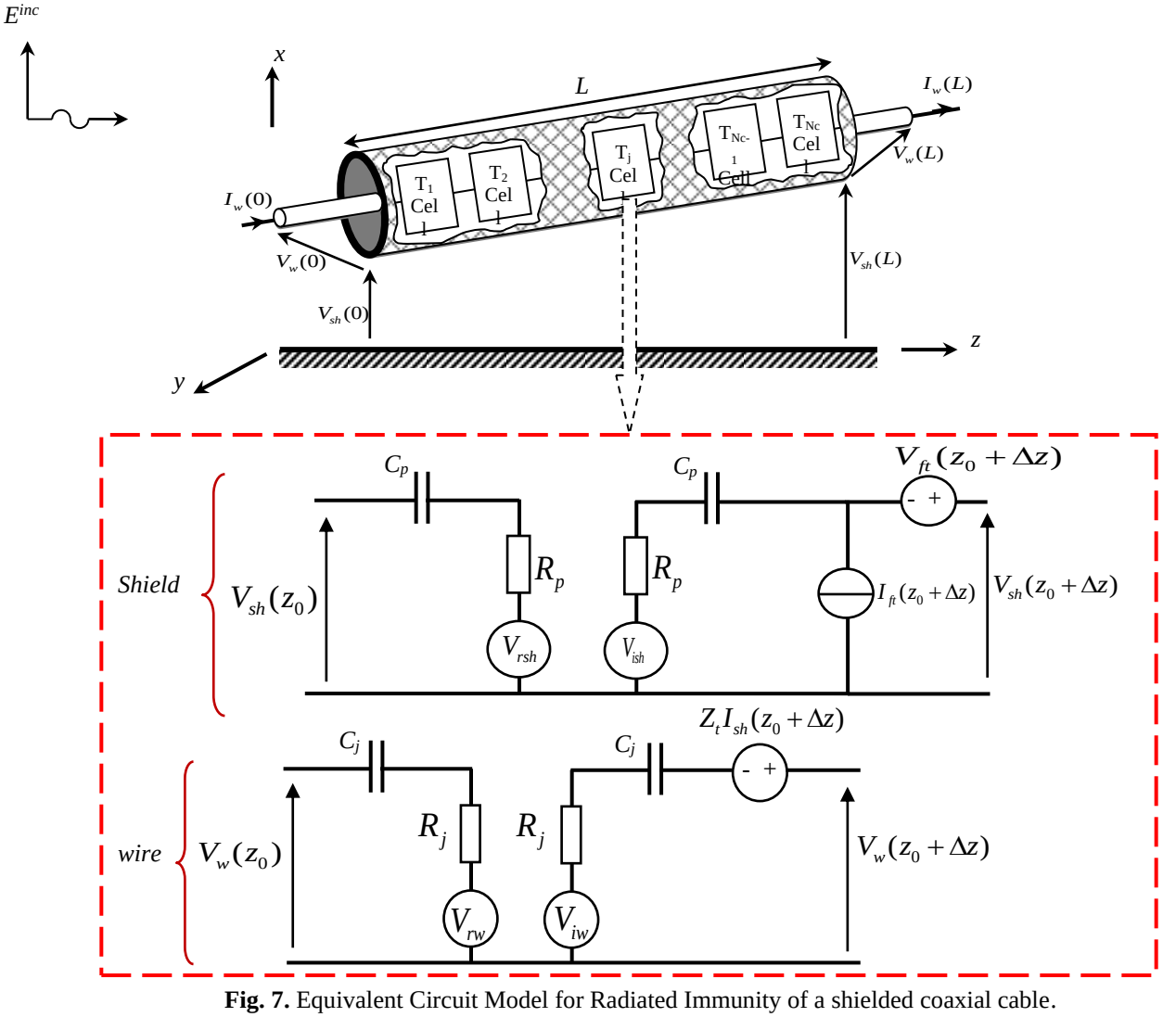

Fig. 7. Equivalent Circuit Model for Radiated Immunity of a shielded coaxial cable.

$$V_{FT}(z_0+\Delta z)=\int_{z_0}^{z_0+\Delta z}\begin{bmatrix}\varphi_{sh11}(\Delta z+z_0-\tau)V_f(\tau)\\+\varphi_{sh12}(\Delta z+z_0-\tau)I_f(\tau)\end{bmatrix}d\tau \quad (20)$$

$$I_{FT}(z_0+\Delta z)=\int_{z_0}^{z_0+\Delta z}\begin{bmatrix}\varphi_{sh21}(\Delta z+z_0-\tau)V_f(\tau)\\+\varphi_{sh22}(\Delta z+z_0-\tau)I_f(\tau)\end{bmatrix}d\tau \quad (21)$$

Where, $\varphi_{sh11}(\Delta z)$, $\varphi_{sh21}(\Delta z)$, $\varphi_{sh22}(\Delta z)$ and $\varphi_{sh12}(\Delta z)$ are the elements of the chain parameter matrix, defined as

$$\varphi_{Sh11}(\Delta z)=\varphi_{Sh22}(\Delta z)=Cosh(\gamma_{sh}\Delta z)=\frac{e^{\gamma_{sh}\Delta z}+e^{-\gamma_{sh}\Delta z}}{2} \quad (22)$$

$$\varphi_{Sh12}(\Delta z)=-Sinh(\gamma_{sh}\Delta z)Z_{csh}=-Z_{csh}\frac{e^{\gamma_{sh}\Delta z}-e^{-\gamma_{sh}\Delta z}}{2} \quad (23)$$

$$\varphi_{Sh21}(\Delta z)=-\sinh(\gamma_{sh}\Delta z)Z_{csh}^{-1}=-Z_{csh}^{-1}\frac{e^{\gamma_{sh}\Delta z}-e^{-\gamma_{sh}\Delta z}}{2} \quad (24)$$

3. SIMULATION RESULTS AND VALIDATION

3.1. Conducted Susceptibility Analysis

In order to validate this model, some simulations have been carried out. Considering a coaxial cable over a ground plane as shown in Fig. 8, the height of the cable over the ground h and the length L are 1cm and 1m, respectively. The inner wire radius r_w and the shield radius r_s are 0.25mm and 2,5mm, respectively. The relative permittivity is $\varepsilon_r = 2{,}375$. The value of the transfer impedance is: $R_T = 100\text{m}\Omega/\text{m}$ and $L_T = 0.5\text{nH/m}$. The terminal loads are given by $R_{s1} = 1\text{G}\Omega$, $R_{s2} = 154{,}363\Omega$ and $R_{w2} = R_{w1} = 44{,}012\Omega$.

The lumped current source embraced for the transient analysis is a clock wave of unit amplitude characterized by period $T_{clk} = 20\text{ns}$, rise and fall time, and duty cycle $\tau/T_{clk} = 0{,}5$. Fig. 9 demonstrates the wire-to-shield voltage at the cable ends which is achieved by the proposed model, accompanied by the results obtained by the compact circuit model suggested in [3] and by the Finite Difference Time Domain (FDTD) method. The achieved results are in very good agreement with those previously obtained using the above mentioned models and methods.

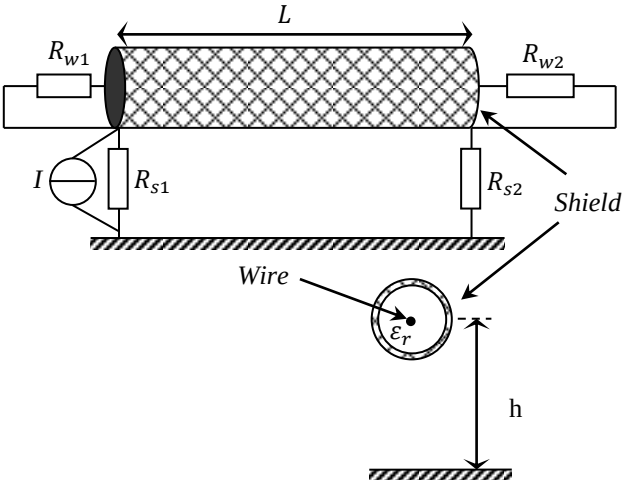

Fig. 8. Configuration adopted of the simulation for conducted susceptibility analysis.

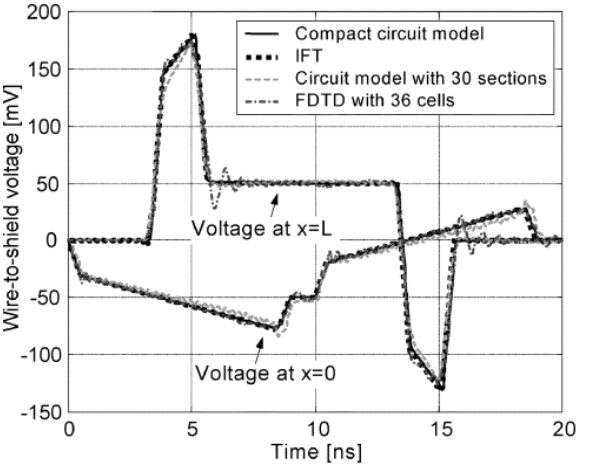

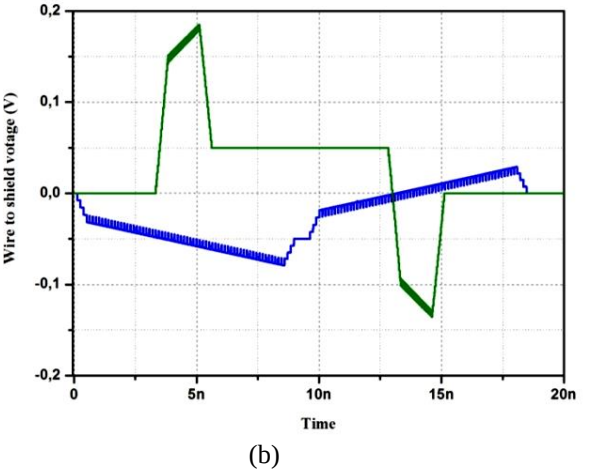

(b)

Fig. 9. Voltage responses of the inner loads in the transient analysis obtained by (a) the proposed model (b) different methods [3].

3.2. Radiated Susceptibility Analysis

The examination of the emanated immunity is carried out on the coaxial cable as appeared in Fig. 10. The shielding radius and the inner wire radius are 0,25mm and 0,108mm, respectively. The cable's characteristic impedance is $Z_c = 50\Omega$, and the relative permittivity ε_r of the internal dielectric filling is 1,77. The value of the transfer impedance is set to $R_T = 1\Omega/m$ and $L_T = 0H/m$. The height h and the length L are 5,25mm and 1m, respectively. The internal conductor is adapted with $R_{w1}= R_{w2}= =50\Omega$. The external field oriented along x and propagating along z axis (E_x–K_z) has amplitude E=1V/m. The shield is short circuited on the right (R_{S2} =0.5 Ω).

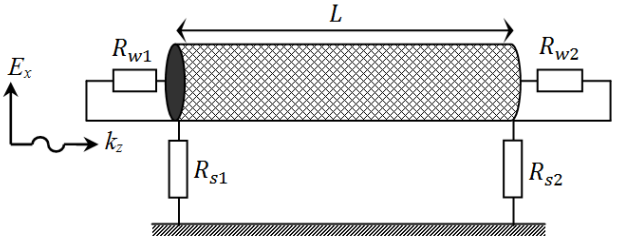

Fig. 10. Configuration adopted of the simulation for radiated susceptibility analysis.

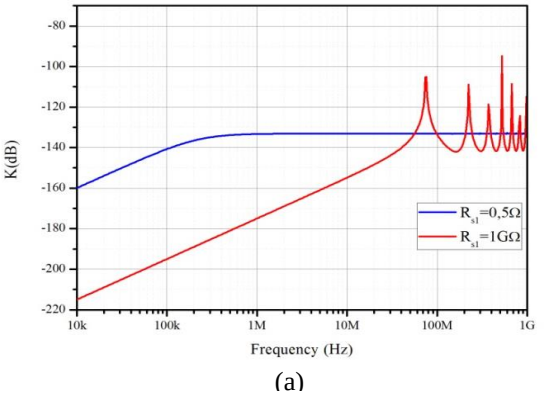

(a)

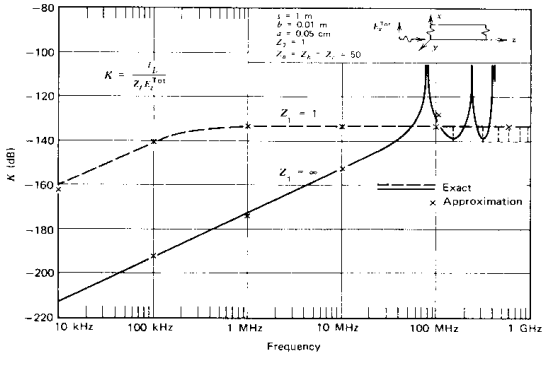

(b)

Fig. 11. Current induced on coaxial cable in dBA obained by the proposed model (a) and analytical method (b)[6] (normalized to $Z_t E_z^{Tot}$)

We recover the current into Dba, at the output of the coaxial cable, which is matched with the same results published by Smith [6], as shown in Fig.11. In addition, it is crystal clear that the line resonates at $f_n = n\left(3\times10^8/\lambda\right)$, n=1, 3, 5… (f_1=75MHz, f_2=225MHz, f_3=375MHz…), when it is loaded with short circuit at far-end and open circuit at near-end. The cable shield should be grounded at both ends in order to eliminate the coupling to internal wire.

3.3. Radiated Susceptibility Analysis of Nonuniform Coaxial Cable

Considering a lossy and nonuniform shielded coaxial cable of 1m length above a perfectly conducting ground plane (PEC), and excited by an incident plane wave, as illustrated in Fig. 12. The inner wire radius r_w and the shield radius R_{sh} are 0,108mm and 0,25mm, respectively. The cable's characteristic impedance is Z_c =50Ω, with dielectric constant ε_r = 1,77. α that is the angle between the cable and the ground plane. The value of the transfer impedance is set to R_T =1Ω/m and L_T = 0H/m. The terminations of the wire are R_1 = 50Ω and R_2 =50Ω. The external field oriented along x and propagating along z axis ($E_x - k_z$) has amplitude E=0,5V/m.

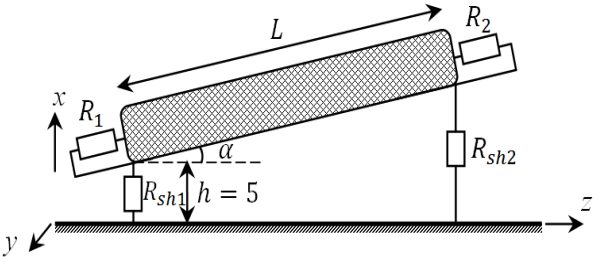

Fig. 12. Nonuniform Coaxial shielded cable over a perfectly conducting ground.

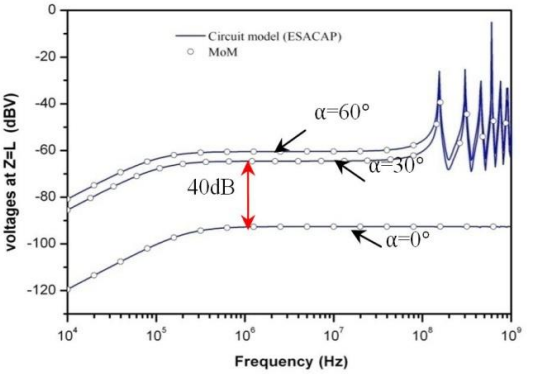

Fig. 13. Far-end voltages for coupled nonuniform shielded coaxial cable for R_{sh1}=R_{sh2}=1Ω.

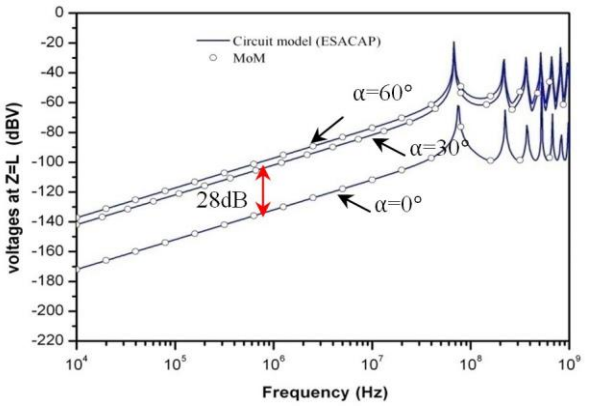

Fig. 14. Far-end voltages for coupled nonuniform shielded coaxial cable for R_{sh1}=1GΩ & R_{sh2}=1Ω.

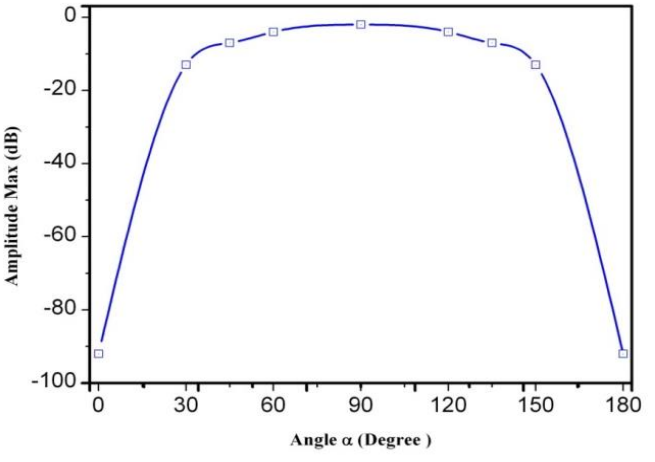

Fig. 15. Maximum amplitude variation as a function of the angle α for R_1=R_2= 50 Ω.

It is observed that in all cases, the line resonates at $f_n = n\left(3 \times 10^8/\lambda\right)$, n=1, 3, 5… (f_1=75MHz, f_2=225MHz, f_3=375MHz…), when the shield load is open at the near-end. The value chosen here of the open circuit resistance is 1GΩ. However, the line resonates at $f_n = n\left(3 \times 10^8/\lambda\right)$, n=2,4,6…(f_1=150MHz, f_2=300MHz, f_3=450MHz…), with the presence of a short circuit at the ends. Moreover, It is noted that all resonance are practically removed when α=0, and the internal immunity is decreased by less than 40dB.

It is noticed from Fig. 15 that the tension is increased when the angle reaches 90°, and it is decreased as the angle leans to 0° and 180°. Therefore, it is observed that there is an asymmetry when the angle is 90°.

3.4. Radiated Susceptibility Analysis of Complex Configuration of Coaxial Cable

Fig. 16 shows a nonuniform coaxial cable excited by an incident plane wave, while the incident field E = 1V/m. The shield radius R_{sh} and the inner wire radius r_w are 1,5mm and 0,25mm, respectively, with dielectric constant ε_r= 1,77. The length L and the initial height h_1 of the cable are 2m length (T_1=1m, T_2=0,5m and T_3=0,5m) and 1cm, respectively. The loads R_1 and R_2 between the inner wire and the shield at the two terminations are R_1 = 50Ω and R_2 = 50Ω. The value of the transfer impedance is set to R_T = 0,01Ω/m and L_T =1nH/m.

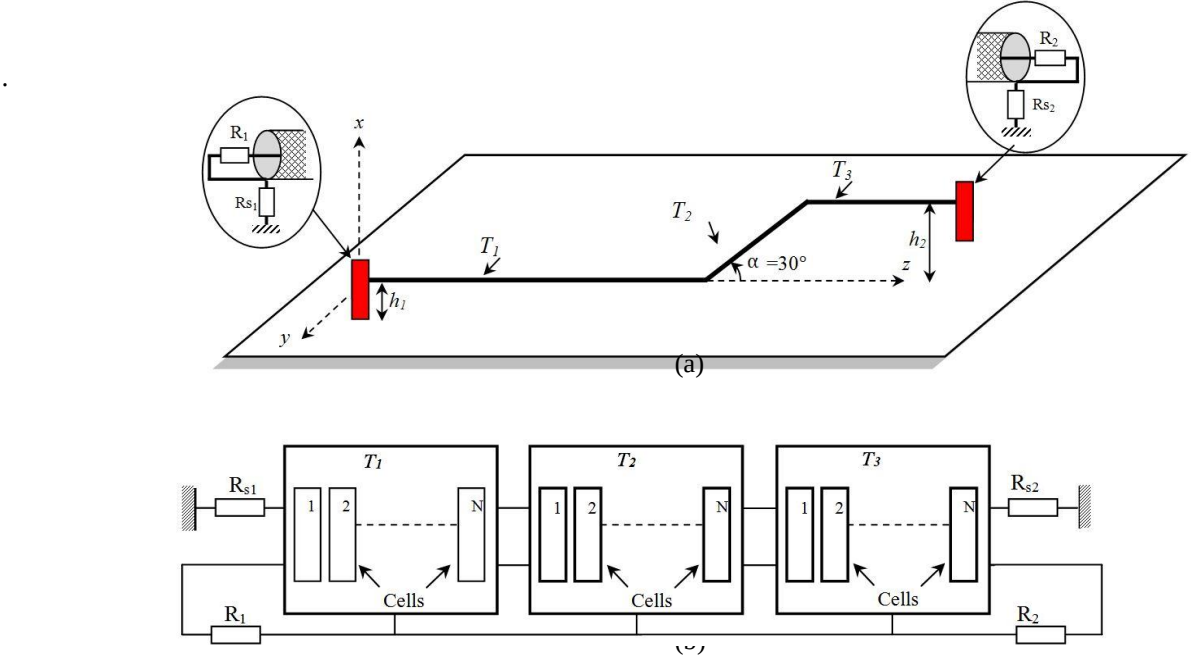

Fig. 16. (a) A nonuniform shielded coaxial cable excited by an incident field (b) Electrical schema used for simulation.

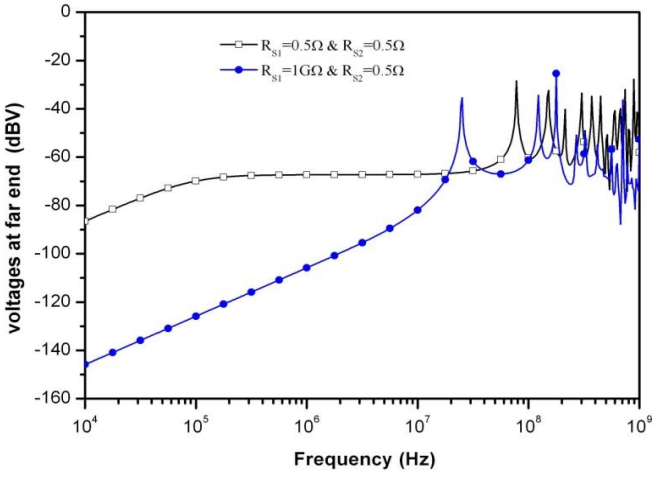

Fig. 17. The voltages at the loads of far-end.

Fig. 17 demonstrates the voltages at loads of far-end and near-end of the inner wire induced by external fields. The simulation results confirm that the best solution for low-frequency disruptions is the grounding of the cable shield on just one side. In addition, due to the cable resonances high disruption tops occur at high frequencies. The suggested circuit models display the following advantages: They can be applied in both the frequency and time domains, and the Inverse Fourier Transform (IFT) is not required to get the time domains outcomes.

4. CONCLUSION

The main purpose of this paper is to present equivalent circuit models of nonuniform shielded coaxial cables to analyze the radiated susceptibility. First, the cable is subdivided into several uniform sections. Second, the voltage and current distributions are determined by using Branin's model. Furthermore, the main advantage of these models is the ability to be used directly in time and frequency domain analysis. It should be noted, as well, that the proposed circuit model is also used for linear and nonlinear loads. To sum up, it is possible to extend the models to nonuniform, multiconductor shielded cables. This question will be further discussed in more details in the next study.

REFERENCES

[1] Z. Bouzidi, A. El Idrissi, H. Rouijaa, and M. Saih, **"Transmission Lines Modeling Approach Based on the Approximation of Pade, "**, presented at PhotonIcs & Electromagnetics *Research Symposium - Spring (PIERS-Spring)*, pp. 4009–4017, Rome, Italy, Jun. 2019.

[2] S. Caniggia and F. Maradei, **"Equivalent circuit models for the analysis of coaxial cables immunity,"** *IEEE Symposium on Electromagnetic Compatibility*. vol. 2, pp. 881–886, Aug. 2003.

[3] S. Caniggia and F. Maradei, **"SPICE-Like Models for the Analysis of the Conducted and Radiated Immunity of Shielded Cables,"** *IEEE Trans. Electromagn. Compat.*, Vol. 46, No. 4, pp. 606–616, Nov. 2004.

[4] H. Xie, J. Wang, R. Fan, and Y. Liu, **"Spice models for radiated and conducted susceptibility analyses of multiconductor shielded cables,"** *Prog. Electromagn. Res.*, Vol. 103, pp. 241–257, 2010.

[5] H. Xie, J. Wang, R. Fan, and Y. Liu, **"SPICE Models to Analyze Radiated and Conducted Susceptibilities of Shielded Coaxial Cables,"** *IEEE Trans. Electromagn. Compat.*, Vol. 52, No. 1, pp. 215–222, Feb. 2010.

[6] M. Saih, H. Rouijaa, and A. Ghammaz, **"Circuit models of lossy coaxial shielded cables connected to non-linear loads to analyze radiated and conducted susceptibilities,"** *Int. J. Microw. Wirel. Technol.*, Vol. 9, No. 7, pp. 1489–1497, Sep. 2017.

[7] M. Saih, H. Rouijaa, and A. Ghammaz, **"Circuit models of multiconductor shielded cables: incident plane wave effect: Incident Plane Wave Effect,"** *Int. J. Numer. Model. Electron. Netw. Devices Fields*, Vol. 29, No. 2, pp. 243–254, Mar. 2016.

[8] M. Raya and R. Vick, **"SPICE Models of Shielded Single and Multiconductor Cables for EMC Analyses,** *IEEE Trans. Electromagn. Compat.,.*, Vol. 62, No. 4, pp. 1563–1571, Aug. 2020.

[9] Z. E. Mohamed Cherif *et al.*, **"Transfer Impedance Measurement of Shielded Cables Through Localized Injection,"** *IEEE Trans. Electromagn. Compat.*, Vol. 60, No. 4, pp. 1018–1021, Aug. 2018.

[10] A V. Cooray, M. Rubinstein, and F. Rachidi, **"Field-to-Transmission Line Coupling Models With Special Attention to the Cooray–Rubinstein Approximation,"** *IEEE Trans. Electromagn. Compat.*, pp. 1–10, 2020.

[11] M. Stumpf and G. Antonini, **"Electromagnetic Field Coupling to a Transmission Line—A Reciprocity-Based Approach,"** *IEEE Trans. Electromagn. Compat.*, Vol. 62, No. 2, pp. 461–469, Apr. 2020.

[12] S. Mashayekhi and B. Kordi, **"Fast and efficient calculation of lightning-induced voltages in frequency-dependent transmission lines over lossy ground,"** *Electr. Power Syst. Res.*, Vol. 98, pp. 19–28, May 2013.